

Dynamics of drop formation in granular suspensions: the role of volume fraction

T. Bertrand · C. Bonnoit · E. Clément · A. Lindner

Received: 11 August 2011 / Published online: 25 January 2012
© Springer-Verlag 2012

Abstract The presence of grains strongly modifies the detachment of drops of a viscous liquid. We have shown previously that the detachment of drops of granular suspensions takes place via different regimes (Bonnoit et al. submitted, 2011). Here we study the influence of the volume fraction of particles on the formation and shape of the droplets by means of visual observations. We measure the minimal neck diameter as well as the height of the detachment as a function of time to quantify the evolution of the drop shape. We also address the question of the thinning dynamics of the neck in the different regimes. Linking the dynamics to the properties of the effective fluid or to rearrangements of individual grains in the thread gives insights in the origin of the different regimes.

Keywords Drop detachment · Granular suspension

1 Introduction

The stability of jets or the detachment of drops is an important issue in everyday life as well as industrial applications. The formation of drops can be important for simple liquids, complex fluids or even dense suspensions or pastes. Especially in the food industry concentrated suspensions or pastes are processed, extruded from nozzles or filled in recipients. The

formation of drops of liquids laden with particles is of great importance for example for inkjet printing [1].

Following a study by Furbank et al. [2, 3] we have recently shown that the presence of grains strongly modifies the detachment of drops of granular suspensions. We have shown that the detachment takes place via different regimes and we have characterized the crossover between these regimes as a function of the volume fraction and the grain diameter [1]. Here we study the influence of the volume fraction of particles on the formation and the shape of the droplets by means of visual observations. We measure the minimal neck diameter as well as the height of the detachment as a function of time to quantify the evolution of the drop shape. We also address the question of the thinning dynamics of the neck in the different regimes.

The paper is organized as follows. In Sect. 2, we introduce our model suspensions and give their properties under shear and elongation. We recall previous observations made on the different detachment regimes observed during drop formation of granular suspensions. Section 3 contains the main findings of this paper. We discuss the drop shape as a function of the volume fraction, the evolution of the shape during the detachment process and zoom on the thinning dynamics in the different detachment regimes. We conclude in Sect. 4.

2 Granular suspensions: background

2.1 Granular model suspensions

We use model suspensions formed by spherical polystyrene beads Dynoseeds from Microbeads with typical grain diameters from $d = 20$ to $140 \mu\text{m}$ and different volume fractions $\phi = V_g / V_0$, defined as the volume of grains V_g on the total

T. Bertrand · C. Bonnoit · E. Clément · A. Lindner (✉)
PMMH-ESPCI, 10, rue Vauquelin, 75231 Paris Cedex 05, France
e-mail: anke.lindner@espci.fr

Present Address:

T. Bertrand
Department of Mechanical Engineering and Materials Science,
Yale University, New Haven, CT 06520-8286, USA

Table 1 Table of the viscosities at 21°C—the viscosities of the suspensions are calculated from the Zarraga model

| Suspensions (%) | η_{Susp} (Pa.s) | Pure oils | η_{PO} (Pa.s) |
|-----------------|----------------------|-----------------|--------------------|
| | | SE (η_0) | 0.18 |
| $\phi = 15$ | 0.29 ± 0.01 | AP200 | 0.26 |
| $\phi = 40$ | 1.55 ± 0.1 | AP1000 | 1.4 |
| $\phi = 50$ | 7.6 ± 0.8 | Sylgard | 6.5 |

The error is due to an uncertainty of $\phi \pm 1\%$. The viscosities of the pure oils have been measured by classical rheometry

volume V_0 . The grains are dispersed in a silicon oil (Shin Etsu SE KF-6011) closely matching their density. The viscosity of the pure oil is $\eta_0 = 0.18$ Pa.s and its surface tension $\gamma = 21 \pm 1$ mN m⁻¹ at $T = 21^\circ\text{C}$. Our suspensions can be qualified as monodisperse, non-buoyant suspensions, where Brownian motion can be neglected.

2.2 Granular suspensions under shear

Shear viscosity—The shear properties of suspensions have been extensively studied [4], but determining the shear viscosity using classical rheology still often fails [5]. In a previous study [6, 7] we have characterized the shear viscosity of our model suspensions combining inclined plane and classical rheometry. We have shown that in a certain range of parameters the suspensions behave as Newtonian fluids. The shear viscosity is independent of the shear rate and only function of the volume fraction. This results holds true for all grain diameters tested. The shear viscosity of the suspensions is in this case well described by models such as the Zarraga model [8] $\eta(\phi) = \eta_0 \frac{\exp(-2.34\phi)}{(1-\phi/\phi_m)^3}$ with $\phi_m \approx 0.62$ and η_0 the viscosity of the interstitial fluid. We have shown that on the inclined plane this simple picture breaks down when the layer thickness drops below a given value, function of the volume fraction [6, 7]. This breakdown might be linked to the formation of clusters of grains, and thus to the particulate nature of the suspensions. It is thus a well known phenomenon that suspensions can either behave as an effective fluid (meaning in the same way as a simple fluid of the same shear viscosity) or show more complex dynamics where the individual grains start to play a role.

Shear viscosity of our suspensions—Here we present results for suspensions of three different volume fractions $\phi = 15, 40$ and 50% with shear viscosities ranging from $\eta_{susp} = 0.29$ –7.6 Pa.s. We also use pure oils AP200 and AP1000 from Sigma Aldrich and Sylgard from Dow Corning matching approximately the viscosities of the suspensions (see Table 1). The surface tension of the pure oils is 20 mN m⁻¹ at $T = 21^\circ\text{C}$. In the following, comparing our results between the suspensions and the pure oils will allow

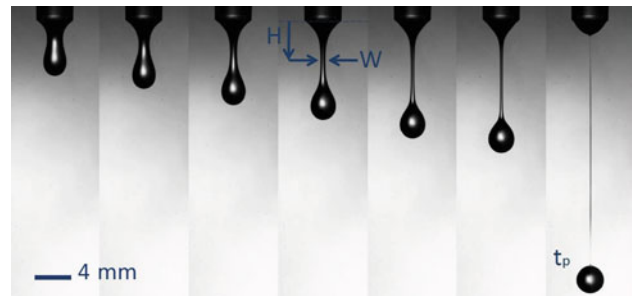


Fig. 1 Typical observations during drop formation of a pure oil (here Shin Etsu). The minimal neck diameter W and the distance H of the minimal neck diameter from the nozzle are measured as a function of time t . t_p denotes the moment of final pinch off

us to precisely answer the question, whether our suspension behave as an effective fluid or not.

2.3 Granular suspension under elongation

Elongational viscosity—During drop formation, the thin thread that links the drop to an outlet undergoes strong elongation (see Fig. 1). The thinning dynamics of this thread are by now well understood for simple fluids [9, 10] and capillary breakup is used as a rheological technique to access elongational viscosities [11]. It has been shown that these viscosities can be strongly increased for complex fluids [12–14].

A typical experiment consists in the extrusion of a liquid from a nozzle and the observation of the subsequent drop formation. One measures the minimal neck diameter W as a function of time t (Fig. 1). For a pure viscous fluid the decrease of W with t takes place via three different stages, characterized by an exponential regime followed by two linear regimes of different slope. The thinning dynamics in these regimes are entirely given by the viscosity and the surface tension of the liquids. Usually one uses the moment of final pinch off t_p as a temporal reference, but strictly speaking this is relevant only for the last regime before final detachment and there is no absolute reference in time for the other detachment regimes. To be able to compare the dynamics far away from the final pinch it might be necessary to use another reference in time instead of t_p as we will also do for some of our analysis.

Elongational viscosity of our suspensions—We have used drop formation of granular suspensions to access their properties under elongation. For these experiment the liquid is filled in a syringe and manually extruded from the latter. The outer diameter of the nozzle is 4 mm, corresponding to the initial size of the drop. We record images with a fast camera at a frame rate of 4,000 fps and a resolution of 1,024*256 pixels (more details can be found in [1]). Image processing with ImageJ is used to extract the profiles of the drops. For all experiments we determine the minimal neck diameter W

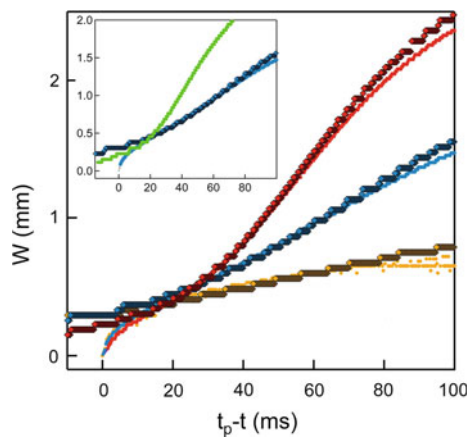


Fig. 2 W as a function of $t_p - t$ for $d = 40 \mu\text{m}$ volume fractions $\phi = 15\%$ (red), 40% (blue) and 50% (orange) and the corresponding oils AP200, AP1000 and Sylgard. The oils are indicated as the diamonds, the suspensions as the dots. The origin of the x axis is given by the time of the pinch for the suspension, AP200 and AP1000 plots are shifted in time. Inset W as a function of $t_p - t$ for $\phi = 40\%$ and the pure oil AP1000 (blue) and the interstitial fluid (green). The origin of the x axis is given by the time of the pinch for the suspension, AP1000 and SE plots are shifted in time

and the distance H of the minimal neck diameter from the nozzle as a function of time t . Figure 2 shows W as a function of $t_p - t$ for three different volume fractions and a grain diameter of $d = 40 \mu\text{m}$. Note that when representing the results as a function of $t_p - t$ the time goes from right to left. The results obtained for the suspensions are compared to the pure oils matching their shear viscosity on the same figure.

One observes that in the beginning of the detachment, the dynamics are identical for the suspensions and the corresponding silicon oils. This shows that there is a regime where the dynamics in an elongational flow of a granular suspension are solely given by the effective shear viscosity of the suspensions. This agreement also holds for other grain diameters (data not shown) as long as the grains are not too big ($d < 250 \mu\text{m}$). Our experiments indicate in this way that the elongational viscosity η_e of model suspensions is solely given by the shear viscosity η , as for Newtonian fluids where $\eta_e = 3\eta$, up to the limit of very dense suspensions ($\phi = 50\%$). This observation is in agreement with the results by Furbank et al. [2,3] obtained using a different method.

At a certain stage of the detachment the thinning dynamics start to differ between the suspensions and the pure oils and the evolution of W with time becomes independent of the initial volume fraction. This represents the crossover to another detachment regime.

Different detachment regimes during drop formation of granular suspensions—We have previously shown that the detachment of granular suspensions takes place via a number of different regimes [1]. The inset of Fig. 2 summarizes our findings. It shows W as a function of $t_p - t$ for the suspension of $\phi = 40\%$ together with the results of the pure oil matching

the shear viscosity of the suspension and the interstitial fluid. In the early stages of the detachment the dynamics are identical between the suspension and the pure oil, representing the effective fluid regime, introduced in the previous paragraph. Then one observes a crossover to a regime, where the dynamics are entirely given by the properties of the interstitial fluid. The final detachment is further accelerated compared to the interstitial fluid. The crossover between the different regimes is function of the volume fraction and the size of the particles [1].

3 Dynamics of drop formation

The experiments presented in this paragraph are performed with the setup introduced in Sect. 2.3. We use the three volume fractions $\phi = 15, 40$ and 50% and a grain diameter of $d = 140 \mu\text{m}$.

3.1 Drop shape as a function of volume fraction

From Fig. 1 one can see that the detachment of a drop of a simple viscous fluid, takes place via the formation of a long and stable filament, that continuously thins until final detachment. The more viscous the fluid, the longer and more stable the filament [10]. Here we study the shape of the drops of our suspensions, comparing different volume fractions. In Fig. 3 snapshots of drops are presented at identical neck diameters (as indicated in Fig. 4) for the different volume fractions.

One observes that the higher the volume fraction, the closer to the nozzle the final pinch off takes place. This is opposite to what is observed in simple fluids, when increasing the shear viscosity. The presence of grains seems to prevent the formation of a long and stable filament. In more detail, for large W the form of the drops is comparable for the different volume fractions. Then, the thinning becomes more and more localized for the higher volume fractions, whereas for the small volume fraction one still observes the formation of a filament. Final detachment takes place as the rupture of a thin filament of pure oil (at the limit of our spatial resolution). The length of this filament is very different for the different volume fractions, and is longer for lower volume fractions.

These observations are summarized in Fig. 3 showing the superimposed extracted profiles corresponding to the snapshots. They are also reflected in the measurements of W and H represented in Fig. 4 as a function of $t_p - t$. The higher the volume fraction, the smaller the value of H . For pure oils (measurements not shown) H increases with increasing viscosity. Note also that the position of final detachment is very reproducible for the largest volume fraction, but fluctuates strongly for the smallest volume fraction, indicated by the error bar in Fig. 4.

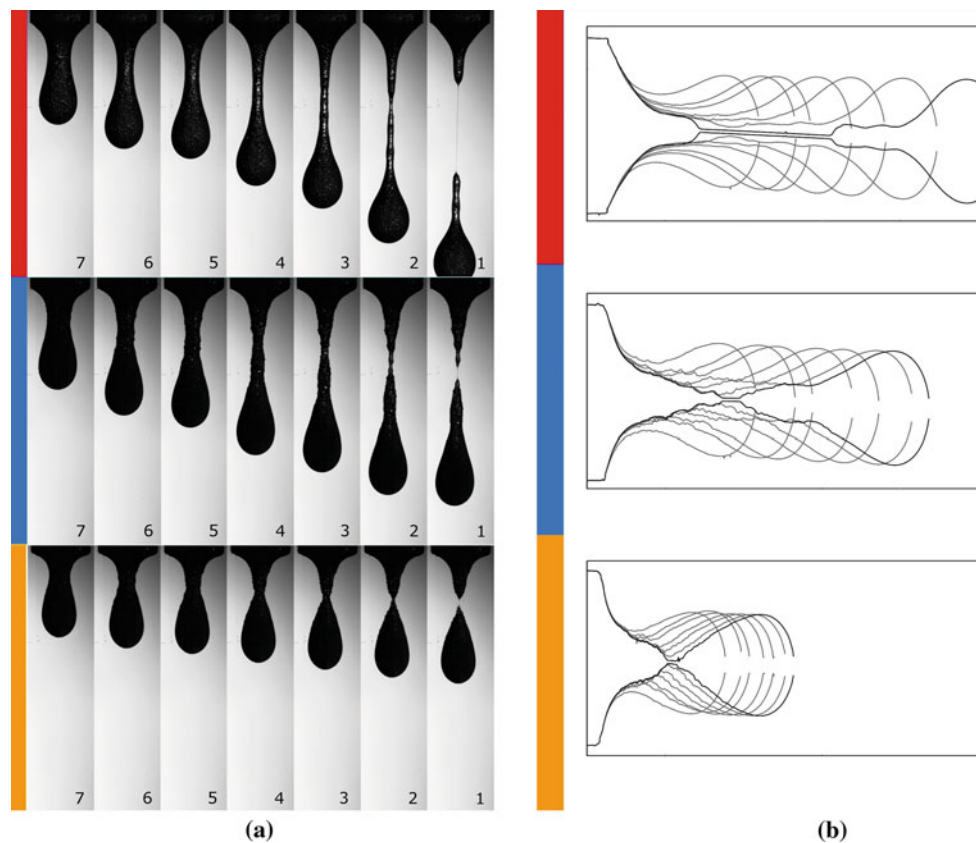


Fig. 3 Drop shape during detachment—**a** snapshots for suspensions of $\phi = 15\%$ (red), 40% (blue) and 50% (orange) and $d = 140 \mu\text{m}$ at fixed neck diameters as given by the dashed lines on Fig. 4. **b** Corresponding profiles, aspect ratio 1 : 1.89

3.2 Evolution of the drop shape during detachment

Visual observations of the evolution of the drop shapes as a function of time (Fig. 3) gives insights in the origin of the different detachment regimes, introduced in Sect. 2.3. For all drops in the beginning of the thinning (snapshots 7,6,5), corresponding to the effective fluid regime, the interface looks smooth and one can not distinguish individual grains.

As the detachment proceeds further (snapshots 4,3) one enters the interstitial fluid regime and one observes that the surface of the drop becomes more and more rough. This is particularly visible for the higher grain fractions. This roughness is of the size of several particles and might be an indication that aggregates of grains form at this stage, leading to local fluctuations of the volume fraction. For the smallest volume fraction these fluctuations can be seen on the snapshots. The resistance to elongation drops dramatically in areas containing less particles and the thinning dynamics become more and more localized at this stage. Finally the thinning dynamics become dominated by the viscosity of the interstitial fluid only. For the higher volume fractions the contrast between

the viscosities of the suspension and that of the interstitial fluid is higher leading to a stronger localization, preventing in this way the formation of a long filament.

Close to the final pinch off, one enters the last detachment regime and a very abrupt decrease in size of the thread is observed (snapshots 2,1). The size of the thread is of the order of a few grain diameters and its size cannot be reduced continuously anymore. This leads to the strong acceleration observed. A small filament of pure interstitial fluid is formed in this way. The length of the filament is longer for less dense suspensions. The relative volume of interstitial oil, being larger for lower volume fractions, might control the length of the filament. For the smallest grain fraction, a long filament of pure interstitial fluid is formed and towards the very end of the detachment one recovers the dynamics of the pure interstitial fluid. The thickness of the thread in this regime is outside our experimental resolution, but from Fig. 4 it is clear that the curve for $\phi = 15\%$ is shifted to the right, corresponding to a slow down of the detachment process very close to the final pinch off. For the higher volume fractions this filament is too short to have a visible effect on the dynamics.

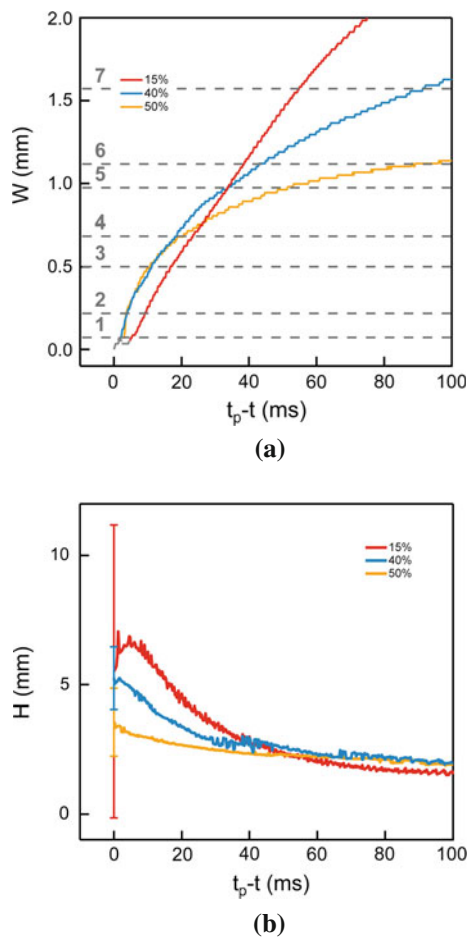


Fig. 4 Minimal neck diameter W (a) and its distance H from the nozzle (b) as a function of $t_p - t$ for $d = 140 \mu\text{m}$ and $\phi = 15\%$ (red), 40% (blue) and 50% (orange)

3.3 Thinning dynamics in the different detachment regimes

In this paragraph we present zooms of the thinning dynamics in the different regimes showing superimposed plots of the contour of the drops. In Fig. 5 the effective fluid regime is shown. The different snapshots are taken at time intervals of $\Delta t = 25$ ms. The interface of the drop is smooth and the thread thins continuously. This is what one would observe for a simple viscous fluid [10]. In Fig. 5 successive profiles at a shorter time interval of $\Delta t = 2.5$ ms are shown in the interstitial fluid regime. It is obvious that structures form and persist in the thread. These structures are larger than a grain size. The thread still thins, but the thinning is more and more localized. As similar observation has been made during detachment of drops of cornstarch [15]. In Fig. 5 the final detachment regime is shown. In this regime the deformation is entirely localized, the form of the drop above and below the minimal neck does not evolve any more. The size of the thread becomes of the order of a few grain sizes, and the thinning is not a continuous process any more. This is more

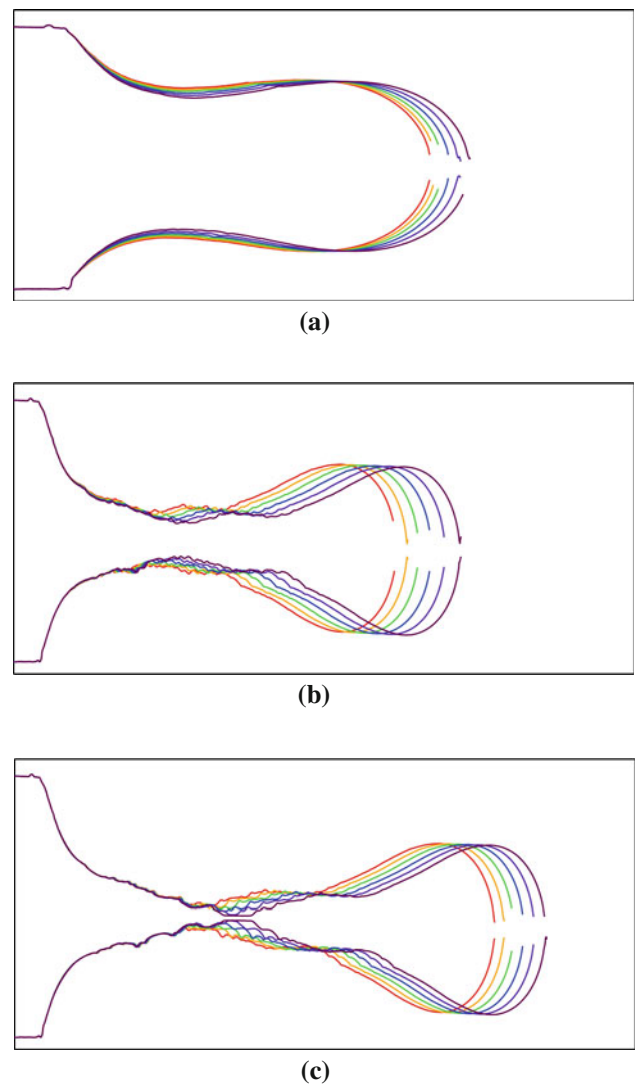


Fig. 5 Drop shape in the different detachment regimes for a suspension of particle of diameter $d = 140 \mu\text{m}$ and volume fraction $\phi = 40\%$. **a** Effective fluid regime—Time step between two successive profiles $\Delta t = 25$ ms, aspect ratio 1 : 1.01. **b** Interstitial oil regime—Time step between two successive profiles $\Delta t = 2.5$ ms, aspect ratio 1 : 1.89. **c** Final detachment regime—Time step between two successive profiles $\Delta t = 1.25$ ms, aspect ratio 1 : 1.89

clearly visible from Fig. 6. The volume of interstitial fluid that is deformed is more and more reduced, leading to the strong acceleration of the detachment observed compared to a filament of pure oil.

4 Conclusion

In this paper we have described the dynamics of the detachment of drops of granular suspensions during extrusion from a nozzle. We have shown that the shape of the drops varies as a function of the volume fraction. For more dense

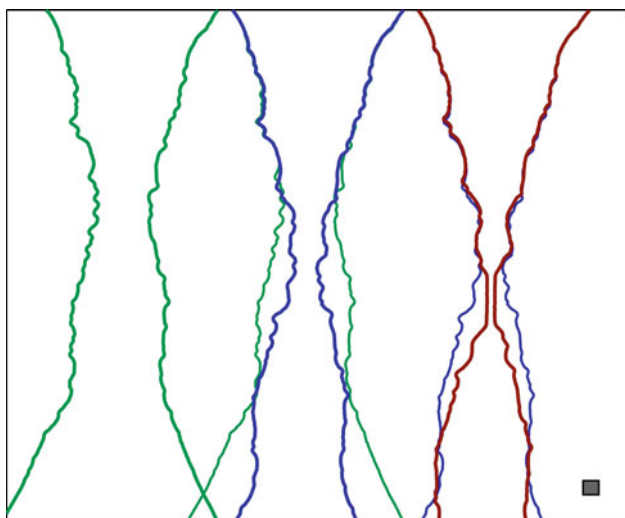


Fig. 6 Zoom on the minimal neck region at different moments of the thinning dynamics, $\Delta t = 1.25$ ms—the square is a scale bar corresponding to $140 \mu\text{m}$, aspect ratio 1 : 0.85

suspensions the detachment takes place closer to the nozzle and the filament linking the drop to the outlet is shorter. This is opposite to what is observed for viscous liquids where more viscous fluids lead to longer and more stable filaments. At the beginning of the detachment process, the dynamics of the suspensions are entirely given by their shear viscosity and they thus behave as an effective fluid. At later stages of the detachment, local fluctuations of the volume fraction are observed. The rearrangement of individual grains can be inferred from the roughness of the surface of the drops that develops at this stage. Locally the neck is freed from grains, leading to a localization of the thinning of the thread, which then becomes governed by the viscosity of the interstitial fluid only. For larger volume fractions the difference in viscosity between the interstitial fluid and the shear viscosity of the suspensions is larger and as a consequence the localization is stronger. Final detachment is very fast. As the thickness of the thread becomes of the size of a few grains no continuous thinning is possible any more. The volume deformed is strongly reduced, leading to the strong acceleration observed. In summary, during formation of drops of

granular suspensions both effective fluid behavior or particulate effects are observed. The interplay between these two limits leads to the specific drop shapes observe for different volume fractions.

Acknowledgments We thank Merlijn van Deen for a critical reading of the manuscript.

References

1. Bonnoit, C., Bertrand, T., Clement, E., Lindner, A.: arXiv:1009.1819v2 (2011, submitted)
2. Furbank, R.J., Morris, J.F.: An experimental study of particle effects on drop formation. *Phys. Fluids* **16**(5), 1777 (2004)
3. Furbank, R.J., Morris, J.F.: Pendant drop thread dynamics of particle-laden liquids. *Int. J. Multiph. Flow* **33**(4), 448 (2007)
4. Stickel, J.J., Powell, R.L.: Fluid mechanics and rheology of dense suspensions. *Ann. Rev. Fluid Mech.* **37**, 129 (2005)
5. Ovarlez, G., Bertrand, F., Rodts, S.: Local determination of the constitutive law of a dense suspension of noncolloidal particles through magnetic resonance imaging. *J. Rheol.* **50**(3), 259 (2006)
6. Bonnoit, C., Lanuza, J., Clement, E., Lindner, A.: Inclined plane rheometry of a dense granular suspension. *J. Rheol.* **54**, 65 (2010)
7. Bonnoit, C., Lanuza, J., Lindner, A., Clement, E.: Mesoscopic length scale controls the rheology of dense suspensions. *Phys. Rev. Lett.* **105**, 108302 (2010)
8. Zarraga, I.E., Hill, D.A., Leighton, D.T.: The characterization of the total stress of concentrated suspensions of noncolloidal spheres in Newtonian fluids. *J. Rheol.* **44**(2), 185 (2000)
9. Eggers, J.: Nonlinear dynamics and breakup of free-surface flows. *Rev. Modern Phys.* **69**(3), 865 (1997)
10. Rothert, A., Richter, R., Rehberg, I.: Formation of a drop: viscosity dependence of three flow regimes. *New J. Phys.* **5** (2003)
11. McKinley, G.H., Tripathi, A.: How to extract the Newtonian viscosity from capillary breakup measurements in a filament rheometer. *J. Rheol.* **44**(3), 653 (2000)
12. Amarouchene, Y., Bonn, D., Meunier, J., Kellay, H.: Inhibition of the finite-time singularity during droplet fission of a polymeric fluid. *Phys. Rev. Lett.* **86**(16), 3558 (2001)
13. Tiratmadja, V., McKinley, G.H., Cooper-White, J.J.: Drop formation and breakup of low viscosity elastic fluids: effects of molecular weight and concentration. *Phys. Fluids* **18**(4) (2006)
14. Sattler, R., Wagner, C., Eggers, J.: Blistering pattern and formation of nanofibers in capillary thinning of polymer solutions. *Phys. Rev. Lett.* **100**(16) 164502 (2008)
15. Roché, M., Kellay, H., Stone, H.A.: Heterogeneity and the role of normal stresses during the extensional thinning of non-brownian shear-thickening fluids. *Phys. Rev. Lett.* **107**, 134503 (2011)